

Diastereoisomers of Platinum(II) Complexes with Chiral *N*-Substituted 1,2-Diamines. I. Structure and Isomerization of Dichloro{(*R*)-2-[(2-methyl-2-aminopropyl) amino]-1-butanol}platinum(II)

Reiko SAITO,[†] Masafumi GOTO,* Junzo HIROSE,^{††} and Yoshinori KIDANI^{†††}

Faculty of Pharmaceutical Sciences, Kumamoto University, Oe Honmachi, Kumamoto 862

[†] Aichi Junior College of Nursing, Kamishidami, Moriyama-ku, Nagoya 463

^{††} Department of Food Science and Technology, Faculty of Engineering, Fukuyama University, Sanzo Higashimura-cho, Fukuyama 729-02

^{†††} Faculty of Pharmaceutical Sciences, Nagoya City University, Tanabe-dori, Mizuho-ku, Nagoya 467

(Received December 20, 1991)

Square-planar complexes with the formula $[\text{PtCl}_2(\text{R-Hb-Mepn})]$, where *R*-Hb-Mepn is (*R*)-2-[(2-methyl-2-aminopropyl)amino]-1-butanol $\text{CH}_3\text{CH}_2\text{CH}(\text{CH}_2\text{OH})\text{NHCH}_2\text{C}(\text{CH}_3)_2\text{NH}_2$, were synthesized and separated into two diastereoisomers. On the basis of CD spectroscopic and X-ray crystallographic analyses, (+)₃₀₀- and (−)₃₀₀-isomers were determined to have the *R*-nitrogen center with λ chelate ring and the *S*-nitrogen center with δ chelate ring, respectively. $R(N)$ - $[\text{PtCl}_2(\text{R-Hb-Mepn})]$ crystallizes in the monoclinic space group $P2_1$ with $a=8.809$ (1), $b=8.9960$ (4), $c=8.536$ (1) Å, $\beta=108.787$ (5)°, $Z=2$, $R=0.042$, and $R_w=0.062$. $S(N)$ - $[\text{PtCl}_2(\text{R-Hb-Mepn})]$ crystallizes in the orthorhombic space group $P2_12_12_1$ with $a=9.287$ (1), $b=14.831$ (1), $c=9.141$ (1) Å, $Z=4$, $R=0.029$, and $R_w=0.034$. ¹H NMR spectra indicate that *R*-Hb-Mepn chelate rings take fixed conformation in acidic D₂O solution. At high temperature (90–95°C), the conversion of the *R(N)*-isomer to the *S(N)*-isomer occurred easily. The $R(N)$ - $[\text{PtCl}_2(\text{R-Hb-Mepn})]$ and $S(N)$ - $[\text{PtCl}_2(\text{R-Hb-Mepn})]$, respectively, show the opposite Cotton effect to that of the reported complexes $R(N)$ - $[\text{PtCl}_2(\text{S-Me-pn})]$ and $S(N)$ - $[\text{PtCl}_2(\text{S-Me-pn})]$ (*S*-Me-pn=(*S*)-1-methylamino-2-aminopropane). The kinetic data of a reversible inversion reaction at the nitrogen were consistent with the usual base catalyzed mechanism.

Interest in the investigation of Pt(II) complexes with *N*-substituted 1,2-diamine arises not only because of their stereochemical properties, but the possibility of their use in antitumor therapy.¹⁾ Coordination of these ligands to Pt(II) ion provides a square-planar complex with an asymmetric secondary nitrogen center. The isolation and structural characterization of Pt(II) complexes with *N*-methyl derivatives of 1,2-ethanediamine or 1,2-propanediamine have been reported.^{2–7)} Concerning *S*-Me-pn Pt(II) complexes (*S*-Me-pn=(*S*)-1-methylamino-2-aminopropane), X-ray structural analyses have been reported for one of the possible isomers.^{4,5)} To our knowledge, there is few reports on the crystal structures of a set of possible diastereoisomers, each of which contains an enantiotopic asymmetric nitrogen center. Crystal structures of *mer*-*RRR*- and *mer*-*RRS*-isomers of tris(*N*-methylethanediamine)cobalt(III) salts have been reported recently.⁸⁾ Analogous complexes with a bulkier substituent on their nitrogen atom(s) have also been only slightly studied.⁹⁾ The main reason for this lack of data on these complexes is due either to the experimental difficulty in isolation of the diastereomers or to their low solubility.

The optical active (*R*)-2-[(2-methyl-2-aminopropyl)amino]-1-butanol (*R*-Hb-Mepn) $\text{CH}_3\text{CH}_2\text{CH}(\text{CH}_2\text{OH})\text{NHCH}_2\text{C}(\text{CH}_3)_2\text{NH}_2$, is a 1,2-propanediamine derivative having a chiral hydroxybutyl group on its nitrogen atom. This ligand can be nominally regarded as a tridentate alcoholic ligand with NNO donor atoms. We selected this *R*-Hb-Mepn ligand aiming that (1) its sterically bulky substituent containing an asymmetric carbon

would facilitate the isolation of the isomers with *R*- and *S*-nitrogen centers and (2) the low solubility of this class of complexes could be improved by the presence of a hydroxyl group.

Several studies on metal complexes with ligands related to *R*-Hb-Mepn have been reported. The compound ethambutol, [*S*-(*R**,*R**)]-[2,2'-(1,2-ethandiyl-di-imino)bis-1-butanol $\text{CH}_3\text{CH}_2(\text{CH}_2\text{OH})\text{CHNHCH}_2\text{CH}_2\text{NHCH}(\text{CH}_2\text{OH})\text{CH}_2\text{CH}_3$, has been widely used as a therapeutic agent because of its remarkably high antituberculin activity.¹⁰⁾ Interactions between ethambutol and metal ions have been investigated from the viewpoint of its biochemical significance.^{11,12)} Divalent metal complexes of the types $[\text{M}(\text{ethambutol})]^{2+}$ (*M*=Co(II) and Ni(II)) and $[\text{M}(\text{ethambutol})_2]^{2+}$ (*M*=Cu(II)) were recently reported.¹³⁾ In the former type complexes the ligand acts as a tetradentate, while in the latter type complex the ligand acts as a bidentate ligand. On the other hand, the ligand 2-((2-aminoethyl)amino)-ethanol (He-en) $\text{CH}_2(\text{OH})\text{CH}_2\text{NHCH}_2\text{CH}_2\text{NH}_2$ coordinates to Pt(II) or Co(III) ion only through the nitrogen atoms.^{14,15)} The resemblance between He-en and *R*-Hb-Mepn suggests that the present *R*-Hb-Mepn is ligated to the Pt(II) ion in a similar fashion as in the He-en complex. Owing to the introduced substituent on the nitrogen, both *R(N)*- and *S(N)*-diastereomers of $[\text{PtCl}_2(\text{R-Hb-Mepn})]$ were easily isolated in high purity and were soluble enough to examine their spectroscopic properties. Here we report the syntheses, properties, and X-ray crystal structure of both isomers.

Experimental

General. The specific rotation was measured using a JASCO DIP-4 polarimeter. The absorption spectra were measured with a Shimadzu UV 210-A spectrophotometer and the CD spectra with a JASCO J600 spectropolarimeter. ^1H NMR spectra were recorded on a JOEL GX-400 spectrometer with D_2O (containing 0.1 mol dm^{-3} DCl and 0.1 mol dm^{-3} KCl) as solvent and sodium 3-(trimethylsilyl)-propionate-2,2,3,3- d_4 (TSP) as an internal reference. The ligand *R*-Hb-Mepn was prepared according to a procedure similar to that for 2-methyl-1,2-diaminopropane but with a slight modification.¹⁶⁾ (*R*)-2-Aminobutanol (Tokyo Kasei) was used without further purification. All reagents used for measuring spectra were of analytical grade.

Preparation of (*R*)-2-[(2-Methyl-2-aminopropyl)amino]-1-butanol (*R*-Hb-Mepn) Dihydrogenchloride. To a solution of 26.7 g (0.3 mol) of (*R*)-2-aminobutanol and 26.7 g (0.3 mol) of 2-nitropropane dissolved in 30 cm^3 of dioxane was added 27 cm^3 of ca. 40% aqueous formaldehyde dropwise at $5\text{--}10^\circ\text{C}$ over 1 h. The mixture was stirred at room temperature for 2 h, then at $65\text{--}70^\circ\text{C}$ for an additional 1 h. Solvents were removed under reduced pressure and the residue was dissolved in 200 cm^3 of ether and the resulting solution was saturated with dry gaseous HCl. The solid obtained was dried over P_2O_5 and NaOH under reduced pressure, then dispersed in $80\text{--}100 \text{ cm}^3$ of acetone and ether (1:1). The precipitate was collected by filtration, washed with ether and dried under reduced pressure, yielding 24.2 g of crude product. The hydrogenation of 16 g of this product in 80 cm^3 of H_2O with 1.4 g of catalyst (5% Pd-C) below 50 atm of hydrogen at 80°C followed by acidification of the diamine obtained with a HCl solution gave 9.1 g of the crude title compound as a dihydrogenchloride salt, which was pure enough to prepare the complexes. An analytical sample was obtained by recrystallization from water. $[\alpha]_{589} = -2.5^\circ$ (5.0 , H_2O). Anal. Found: C, 40.98; H, 9.36; N, 12.01%. Calcd for $\text{C}_8\text{H}_{22}\text{N}_2\text{OCl}_2$: C, 41.21; H, 9.51; N, 12.01%.

Preparation of *R*(*N*)-[PtCl₂(*R*-Hb-Mepn)] (1) and *S*(*N*)-[PtCl₂(*R*-Hb-Mepn)] (2). To a stirred solution of 830 mg (2 mmol) of K_2PtCl_4 and 800 mg (3.4 mmol) of *R*-Hb-Mepn·2HCl in 14 cm^3 of H_2O was added 440 mg (5.2 mmol) of NaHCO_3 . The mixture was allowed to stand overnight at room temperature. Yellow microcrystalline product started to precipitate during the first day. Prism shaped crystals were observed to commence deposition after 2–3 days. The mixture was allowed to stand for 6–7 days to complete precipitation. The product was collected and washed with water and then dried in air to give a mixture of 1 and 2. Typical yield was about 62%.

Separation of 1 and 2. A suspension of 500 mg of the mixture in 9.5 cm^3 of 0.2 mol dm^{-3} AgNO_3 aqueous solution was stirred in the dark for 1 h, the resulting AgCl was removed by filtration and 3 cm^3 of a 1.5 mol dm^{-3} HCl solution then added. After standing in a refrigerator overnight, separated yellow crystals were filtered off, washed with water and dried under reduced pressure yielding ca. 200 mg. The crystals obtained were again treated with AgNO_3 solution to give pure crystals of 1 as microplates. The resulting mother solution was allowed to stand in a refrigerator for 24 h, during which new yellow prismatic crystals appeared. This mixture was concentrated to about 5 cm^3 and then cooled to give about

100 mg of prisms together with a small amount of 1. The crystal mixture was again purified in the same manner as previously described to afford pure crystals of 2 as prisms. 1 and 2 were confirmed to be *R*(*N*)- and *S*(*N*)-[PtCl₂(*R*-Hb-Mepn)], respectively, by X-ray crystallography as will be described later. Anal. Found for 1: C, 22.32; H, 4.50; N, 6.60%. Found for 2: C, 22.83; H, 4.80; N, 6.62%. Calcd for [PtCl₂(*R*-Hb-Mepn)]: C, 22.46; H, 4.73; N, 6.57%.

Preparation of 2 by the Isomerization Reaction of 1. A suspension of 200 mg of 1 in 20 cm^3 of 0.5 mol dm^{-3} LiCl solution was heated at $90\text{--}95^\circ\text{C}$. The less soluble 1 was gradually dissolved, indicating conversion of 1 to the more soluble 2. After the resulting solution was concentrated to ca. 5 cm^3 on a steam bath and cooled to room temperature, ca. 120 mg of yellow prismatic crystals were obtained. A solution of resulting complexes exhibited the same CD spectrum as that of 2.

Equilibrium and Kinetics of Inversion at the Coordinated Secondary Amines. Rate constants and the equilibrium constant of inversion at the nitrogen center of the present diastereomers were determined using complex 1 as the starting material. Complex 1 was dissolved in a 0.04 mol dm^{-3} acetate buffer containing 0.2 mol dm^{-3} KCl. The solution was thermostated at 50.0°C . At appropriate time intervals portions of reaction mixture were withdrawn, cooled to room temperature, and acidified in order to stop the reaction. The CD intensities at 305 nm ($\Delta\epsilon_t$) of each solution were then recorded. For this inversion reaction system the equilibrium was not exactly reached due to slow side reactions, but there arised no serious problem in measuring both $\Delta\epsilon_t$ and $\Delta\epsilon_\infty$. When almost constant CD reading ($\Delta\epsilon_\infty$) was obtained for each run, it was assumed that equilibrium was attained. The equilibrium constant, K_{eq} was estimated using the equilibrium mole ratio of 1 and 2 under the assumption that the $\Delta\epsilon$ values of 1 and 2 at the studied pH is equal with that obtained in acidic medium, respectively. Calculation of the rate constants were carried out using a least-squares method.

Collection and Reduction of X-Ray Data. Sample crystals of 1 for X-ray diffraction were obtained in the following method. They were crystallized from the filtrate of the AgNO_3 treated mixture of an aqueous solution of 1 by very slow addition of a diluted HCl solution. Sample crystals of 2 could be easily obtained without particular attention. X-ray data were collected by mounting each single crystal on a glass capillary in an Enraf-Nonius CAD4 diffractometer. Cell dimensions were calculated from automatically centered reflections. The data were corrected for absorption empirically and Lorentz-polarization. The absorption correction was based on an azimuthal (ϕ) scan of 3 (for 1) or 2 (for 2) reflections. Three check reflections were monitored every 2 h during acquisition time. For 1 no significant deviation occurred. For 2 a linear correction for decay was applied. Crystal and empirical data are summarized in Table 1.

Solution and Refinement of the Structures. The structures were solved and refined using the Enraf-Nonius SDP crystallographic computing package.¹⁷⁾ In each case platinum atoms were located by the heavy atom method from a Patterson map and the remaining non-hydrogen atoms were found from subsequent Fourier syntheses. They were refined anisotropically. All hydrogen atoms were fixed in calculated positions. Atomic scattering factors and anomalous dispersion terms were taken from the usual sources.¹⁸⁾ The absolute configuration of

Table 1. Experimental Data for the X-Ray Diffraction Study

	1	2
Formula	C ₈ H ₂₀ N ₂ Cl ₂ OPt	C ₈ H ₂₀ N ₂ Cl ₂ OPt
Mol wt	426.2468	426.2468
Crystal system	Monoclinic	Orthorhombic
Space group	<i>P</i> 2 ₁	<i>P</i> 2 ₁ 2 ₁ 2 ₁
<i>a</i> /Å	8.809(1)	9.287(1)
<i>b</i> /Å	8.9960(4)	14.831(1)
<i>c</i> /Å	8.536(1)	9.141(1)
β /°	108.787(5)	
<i>V</i> /Å ³	640.4(1)	1259.0(2)
<i>Z</i>	2	4
<i>F</i> (000)	404	808
<i>d</i> _{calcd} /g cm ⁻³	2.210	2.250
<i>d</i> _{obsd} /g cm ⁻³	2.21	2.24
Crystal size/mm	0.15, 0.21, 0.06	0.35, 0.20, 0.13
Color	Yellow	Yellow
Habit	Plate	Prism
Scan type	ω -2 θ	ω -2 θ
Radiation (Å)	Mo <i>K</i> α (0.71073)	Mo <i>K</i> α (0.71073)
Scan range 2 θ /°	3.0–60	2–60
Temp/K	293	293
Data collcd	<i>h</i> , <i>k</i> , \pm <i>l</i>	<i>h</i> , <i>k</i> , <i>l</i>
No. of reflecons	2088	2118
No. of reflecons used in calcn	1811	1866
<i>R</i> ^{a)}	0.042	0.029
<i>R</i> _w ^{b)}	0.062	0.034

a) $R = \Sigma ||F_o| - |F_c|| / \Sigma |F_o|$. b) $R_w = \{\Sigma w(|F_o| - |F_c|)^2 / \Sigma w F_o^2\}^{1/2}$, $w=1$.

each complex was determined as follows. For complex **1**, the additional reflections of 10 Friedel pairs giving a large difference in intensity were measured. The absolute configuration of **1** was deduced from the relation between $F_c(hkl)$ and $F_c(\bar{h}\bar{k}\bar{l})$ and the corresponding $F_o(hkl)$ and $F_o(\bar{h}\bar{k}\bar{l})$. For **2**, the refinement for another enantiomorph was tested in the final stage with non-hydrogen atoms. The enantiomorph with a lower *R* factor ($R=0.038$, $R_w=0.057$) was chosen as the correct solution, the other enantiomorph has $R=0.049$ and $R_w=0.064$. The molecular plots were produced by the program ORTEP.¹⁹⁾ Lists of anisotropic thermal factors, hydrogen atom coordinates, and $F_o - F_c$ tables were deposited as Document No. 8999 at the Office of the Editor of Bull. Chem. Soc. Jpn.

Results and Discussion

Preparation and the Properties of the Complexes.

The reaction between Pt(II) ion and *R*-Hb-Mepn proceeded very slowly. The bulky substituent on the nitrogen atom would have a dramatic effect on the rate of the complex formation. It was completed only after 6–7 days at room temperature to afford a mixture of two crystalline products. Crystals **1** deposited more rapidly than **2** during both formation and purification. Therefore, separation of the two isomers was easily accomplished. It would also be true that the chiral group caused easy separation of the formed diastereomers. The O–H vibration frequencies proved the presence of an uncoordinated hydroxyl group in both complexes (3490 and 3570 cm⁻¹ for **1** and **2**) and the didentate coordination of the ligand. Two diastereo-

mers having the *R*(*N*)- or *S*(*N*)-nitrogen configuration with the *N*-substituent equatorial would be possible for [PtCl₂(*R*-Hb-Mepn)]. Occurrence of isomers with the *N*-substituent axial would be ruled out owing to the steric hindrance between one of the methyl groups on chelate ring carbon and the hydroxybutyl group on nitrogen. The X-ray structural analysis of the two isomers substantiated this assumption.

Crystal and Molecular Structure of *R*(*N*)-[PtCl₂(*R*-Hb-Mepn)] (1**) and *S*(*N*)-[PtCl₂(*R*-Hb-Mepn)] (**2**).** The structures and the atomic labeling schemes for **1** and **2** are shown in Figs. 1 and 2, respectively. The non-hydrogen atomic coordinates, intramolecular bond distances, and the bond angles are listed in Tables 2, 3, and 4, respectively. The bond distances and angles within the *R*-Hb-Mepn ligand for **1** and **2** agree well with the corresponding values found in structurally related ethambutol dihydrogenchloride.²⁰⁾ The structures of coordination sphere for both complexes resemble each other. The coordination around the Pt(II) was square-planar and the ligand coordinated through two nitrogen atoms. The Pt–N distances almost agree with those found in [PtCl₂(en)]²¹⁾ and [PtCl₂L] (L=*N,N'*-disubstituted 1,2-ethanediamine).^{22–25)} For the present complexes, however, the Pt–N(1) distances are slightly longer than the Pt–N(2) distances: 2.084 (3) and 2.085 (5) vs. 2.05 (1) and 2.024 (5) Å for **1** and **2** respectively. This may be attributable to the presence of the bulky substituent on N(1) atom. The bite angles of N(1)–Pt–N(2), of **1** and **2**, are 84.7 (4)° and 83.6 (2)°, respectively,

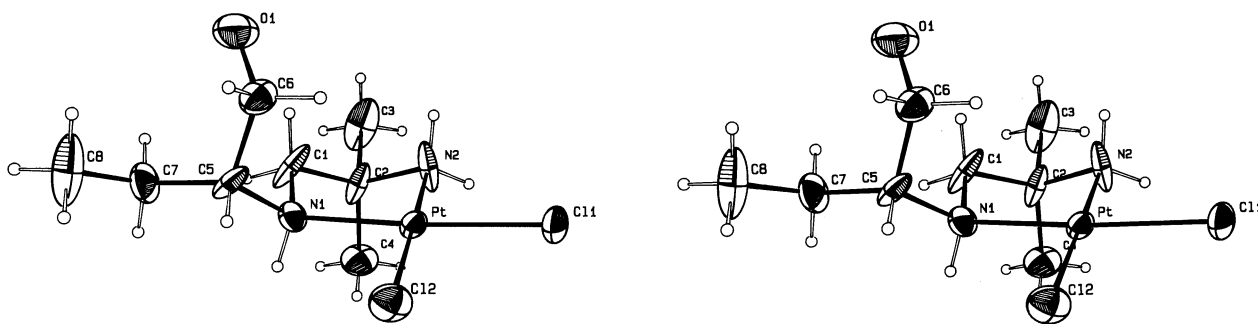


Fig. 1. Stereodrawing of $R(N)$ -[PtCl₂(*R*-Hb-Mepn)] (**1**) and labeling of the non-hydrogen atoms.

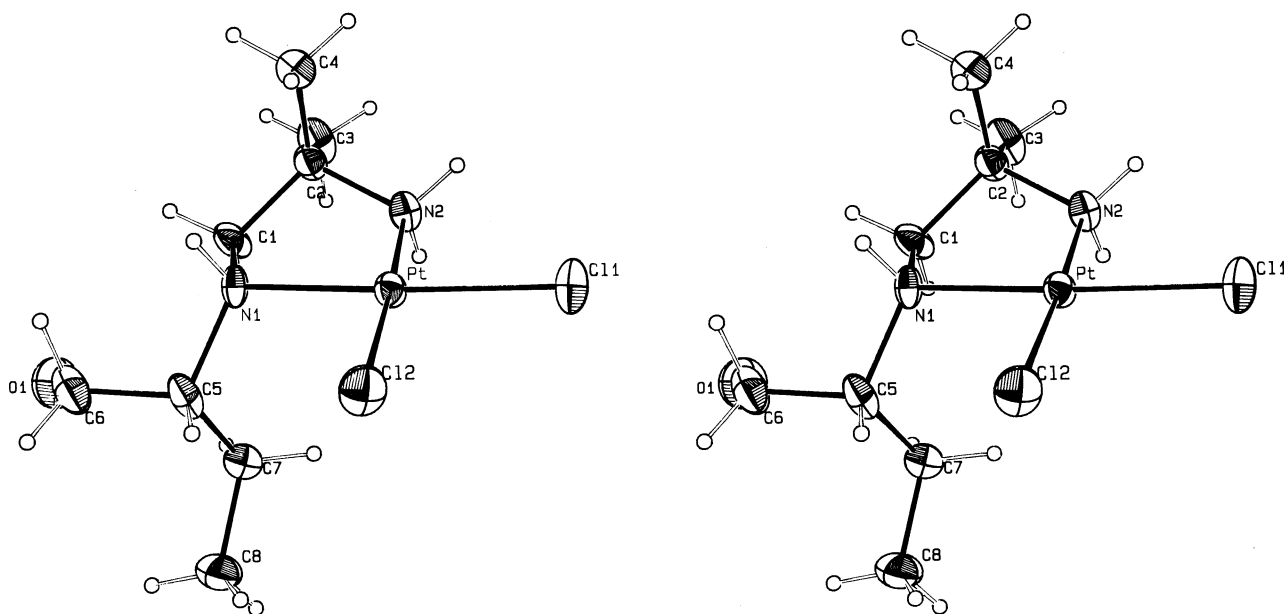


Fig. 2. Stereodrawing of $S(N)$ -[PtCl₂(*R*-Hb-Mepn)] (**2**) and labeling of the non-hydrogen atoms.

and agree with the values observed in other chelate having *S*-Me-pn ligand (83.12 (24)°).⁴⁾ The angles Cl(1)–Pt–Cl(2) of **1** and **2**, which are 91.9 (1)° and 92.03 (8)°, respectively, are close to those reported previously for analogous complexes such as [PtCl₂(*S*-Me-pn)] (92.27 (8)°)⁴⁾ and $R(N),R(N')$ -[PtCl₂(*N,N'*-R₂en)] (R = *R,S*-CHCH₃Ph) (91.2 (1)°).²²⁾ The bite angles of N(1)–Pt–Cl(2), 94.2 (3)° and 94.3 (2)°, are due to the presence of *N*-hydroxybutyl substituents, while the N(2)–Pt–Cl(1) retained normal values: 89.2 (3)° and 90.1 (2)° for **1** and **2** respectively. The chelate rings of the methylpropanediamine are puckered (the torsion angles N(1)–C(1)–C(2)–N(2) are –57 (3)° and 53 (1)° for **1** and **2**,

respectively (Table 5) but unsymmetrically substituted substituent at N(1) causes an rotation of the chelate ring around the N(1)–N(2) direction as to result in the different displacements of C(1) and C(2) from the coordination plane: –0.185 and –0.032 Å for C(1) and 0.600 and 0.626 Å for C(2).

The absolute configuration at the secondary nitrogen atom are *R* and *S* for **1** and **2** respectively and the five-membered chelate rings have λ and δ conformations as required from the dihedral angles of N(1)–C(1)–C(2)–N(2). The substituent bonded to the nitrogen atom has two possible conformations of either axial or equatorial dispositions. Both **1** and **2** have the equatorial

Table 2A. Positional Parameters and Thermal Parameters (\AA^2) of Non H Atoms of $R(N)$ -[PtCl₂(*R*-Hb-Mepn)] with esd's in Parentheses

Atom	<i>x</i>	<i>y</i>	<i>z</i>	<i>B</i> _{eq}
Pt	-0.01898(7)	0.000	-0.01621(6)	1.843(8)
Cl1	-0.1206(7)	0.0781(7)	-0.2890(5)	3.0(1)
Cl2	0.2183(6)	-0.0785(7)	-0.0521(6)	2.9(1)
O1	0.183(2)	0.246(2)	0.422(2)	3.9(4)
N1	0.051(2)	-0.060(2)	0.233(2)	2.1(3)
N2	-0.228(2)	0.068(3)	0.020(2)	3.4(4)
C1	-0.077(2)	-0.004(5)	0.302(2)	3.2(3)
C2	-0.242(2)	-0.023(3)	0.174(2)	2.7(5)
C3	-0.367(2)	0.070(4)	0.233(2)	4.4(6)
C4	-0.289(3)	-0.184(3)	0.128(3)	3.3(5)
C5	0.217(2)	-0.002(4)	0.337(2)	2.4(3)
C6	0.244(3)	0.164(2)	0.316(2)	2.7(4)
C7	0.254(3)	-0.058(3)	0.516(2)	2.8(4)
C8	0.431(3)	-0.039(4)	0.613(3)	5(1)

Table 2B. Positional Parameters and Thermal Parameters (\AA^2) of Non H Atoms of $S(N)$ -[PtCl₂(*R*-Hb-Mepn)] with esd's in Parentheses

Atom	<i>x</i>	<i>y</i>	<i>z</i>	<i>B</i> _{eq}
Pt	0.48527(3)	0.27059(2)	0.49401(4)	1.551(4)
Cl1	0.5672(3)	0.4170(1)	0.5007(4)	2.80(4)
Cl2	0.4021(3)	0.2788(2)	0.7336(3)	2.52(4)
O1	0.493(1)	-0.0807(5)	0.484(1)	4.0(2)
N1	0.4227(9)	0.1367(5)	0.4654(9)	1.8(1)
N2	0.5492(9)	0.2601(5)	0.2830(9)	2.0(1)
C1	0.472(1)	0.1057(6)	0.318(1)	2.4(2)
C2	0.465(1)	0.1845(6)	0.210(1)	2.0(2)
C3	0.546(2)	0.1573(7)	0.070(1)	2.9(2)
C4	0.315(1)	0.2170(8)	0.179(1)	2.9(2)
C5	0.483(1)	0.0742(6)	0.589(1)	2.3(2)
C6	0.418(1)	-0.0200(7)	0.580(1)	2.8(2)
C7	0.645(1)	0.0759(7)	0.596(1)	2.3(2)
C8	0.701(2)	0.0418(8)	0.740(1)	3.3(2)

Table 3. Selected Bond Distances (\AA) in the [PtCl₂(*R*-Hb-Mepn)] Isomers

	1	2
Pt-Cl(1)	2.319(3)	2.301(1)
Pt-Cl(2)	2.318(3)	2.325(2)
Pt-N(1)	2.084(3)	2.085(5)
Pt-N(2)	2.05(1)	2.024(5)
N(1)-C(1)	1.52(2)	1.496(8)
N(1)-C(5)	1.54(2)	1.568(8)
N(2)-C(2)	1.58(2)	1.524(8)
C(1)-C(2)	1.52(1)	1.533(8)
C(2)-C(3)	1.59(2)	1.539(9)
C(2)-C(4)	1.52(2)	1.50(1)
C(5)-C(6)	1.53(3)	1.53(1)
C(5)-C(7)	1.54(2)	1.51(1)
C(7)-C(8)	1.52(2)	1.51(1)
C(6)-O(1)	1.41(2)	1.44(1)

Table 4. Selected Angles ($^\circ$) for **1** and **2**

	1	2
Cl(1)-Pt-Cl(2)	91.9(1)	92.03(8)
Cl(1)-Pt-N(2)	89.2(3)	90.1(2)
Cl(2)-Pt-N(1)	94.2(3)	94.3(2)
N(1)-Pt-N(2)	84.7(4)	83.6(2)
Pt-N(1)-C(1)	107(1)	108.6(4)
Pt-N(1)-C(5)	115(1)	111.9(4)
Pt-N(2)-C(2)	107(1)	108.9(4)
N(1)-C(1)-C(2)	110(1)	109.4(5)
N(2)-C(2)-C(1)	103(1)	104.6(5)
N(2)-C(2)-C(3)	104(1)	107.7(5)
N(2)-C(2)-C(4)	111(1)	108.9(5)
C(1)-C(2)-C(3)	108(1)	108.2(5)
C(1)-C(2)-C(4)	114(2)	114.2(6)
C(3)-C(2)-C(4)	115(1)	112.7(6)
N(1)-C(5)-C(6)	115(1)	111.0(6)
N(1)-C(5)-C(7)	109(1)	112.0(5)
C(6)-C(5)-C(7)	117(1)	114.6(6)
C(5)-C(6)-O(1)	109(1)	114.4(6)
C(5)-C(7)-C(8)	111(1)	111.7(7)

Table 5. Torsion Angles ($^\circ$) for **1** and **2**

	1	2
Pt-N(1)-C(1)-C(2)	38 (3)	-28 (2)
Pt-N(2)-C(2)-C(3)	161 (1)	-162.0 (6)
Pt-N(2)-C(2)-C(4)	-74 (2)	75.6 (8)
Pt-N(1)-C(5)-C(6)	49 (2)	170 (1)
Pt-N(1)-C(5)-C(7)	-179 (2)	-59 (2)
N(1)-C(1)-C(2)-N(2)	-57 (3)	53 (1)
C(5)-N(1)-C(1)-C(2)	164 (2)	-157.9 (9)
N(1)-C(1)-C(2)-C(3)	-167 (2)	167.9 (9)
N(1)-C(1)-C(2)-C(4)	64 (3)	-66 (1)
C(1)-N(1)-C(5)-C(6)	-72 (2)	-65 (2)
C(1)-N(1)-C(5)-C(7)	60 (3)	66 (2)

substituent as indicated by the values of torsion angles C(2)-C(1)-N(1)-C(5), which are $-164 (2)^\circ$ and $158 (1)^\circ$ for **1** and **2**, respectively. The absolute configuration of the carbon atom was confirmed to be *R*, as anticipated by that of the starting material used for the preparation of the ligand. The hydroxybutyl group directs the tertiary proton toward the chlorine atom in *cis*-position in order to release the steric repulsion. The difference between **1** and **2** lies in the dispositions of ethyl and hydroxymethyl group attached to C(5) other than their approximate relationship of the mirror image. The torsion angles of C(1)-N(1)-C(5)-C(6) and C(1)-N(1)-C(5)-C(7) are in the vicinity of $+60^\circ$ and -60° , because the tertiary proton protrudes in the direction of *cis*-chlorine atom in each isomer. The torsion angles of Pt-N(1)-C(5)-C(6) are $49 (2)^\circ$ and $170 (1)^\circ$, while those of Pt-N(1)-C(5)-C(7) are $-179 (2)^\circ$ and $-59 (2)^\circ$ for **1** and **2** respectively. The ethyl part extends approximately in the plane of the coordination plane but the hydroxymethyl part extends approximately in the direction perpendicular to the

coordination plane in **1**. These directions are reversed in **2**.

CD Spectra. The absorption and CD spectra of the two isomers of $[\text{PtCl}_2(\text{R-Hb-Mepn})]$ are shown in Fig. 3. The absorption spectra of both complexes are very similar to those of $[\text{PtCl}_2(\text{S-Me-pn})]$ ^{3,4)} and $[\text{PtCl}_2(\text{S-pn})]$ ($\text{S-pn}=(\text{S})$ -1,2-propanediamine).^{26,27)} The CD curve of the diastereomer **1** was found to be almost enantiomorphous to that of the diastereomer **2**. If we assume that the additivity of the CD contributions holds for these complexes, the vicinal effect of the chiral carbon can be estimated to be much weaker than the sum of the vicinal effects of both the chiral nitrogen and the chelate ring conformation. The $[\text{PtCl}_2\text{L}]$ ($\text{L}=\text{N}$ -substituted diamine) type complexes containing an asymmetric nitrogen center exhibit a considerably intense CD band at ca. 33000 cm^{-1} ,^{3,4)} which has been assigned to the $^1\text{A}_1 \rightarrow ^1\text{A}_2$ transition.²⁵⁾ The same type complex with optically active pn or 1,2-butanediamine derivative did not show such a characteristic band.²⁶⁻²⁹⁾ Studies of X-ray structure of $\text{S}(\text{N})$ - $[\text{PtCl}_2(\text{S-Me-pn})]$ and CD analysis for $\text{S}(\text{N})$ - and $\text{R}(\text{N})$ - $[\text{PtCl}_2(\text{S-Me-pn})]$ have suggested that the complex giving a positive Cotton effect at the $^1\text{A}_2$ band can be assigned to the *S*-nitrogen center or vice versa.^{3,4)} However, our experimental result indicates that this empirical rule was not applicable for all the complexes of this type, $[\text{PtCl}_2\text{L}]$ ($\text{L}=\text{N}$ -substituted diamine). In fact, the present *R*-Hb-Mepn complex with the *S*-nitrogen configuration exhibits the dominant negative CD sign at ca. 33000 cm^{-1} . This suggests that an absolute *R*- or *S*-nitrogen configuration is of no intrinsic importance, because the complex with the same arrangement around the nitrogen is named as "*R*(*N*)" or "*S*(*N*)" depending on the size of the substituent on the nitrogen. It has been well known that the optical activity was generated by the dissymmetric potentials owing to the carbon atom on the donor nitrogen atom. Correlations of the octant sign with the signs of Cotton effect were discussed for various complexes.³⁰⁻³³⁾ As shown in Table 6, $[\text{PtCl}_2\text{L}]$ complexes, whose carbon atom on the asymmetric nitrogen in the *N*-substituent (C_N) is located octant minus region,²⁹⁾ exhibit a positive $^1\text{A}_2$ Cotton effect. For this transition the contribution from the dissymmetric potential due to the chelate ring

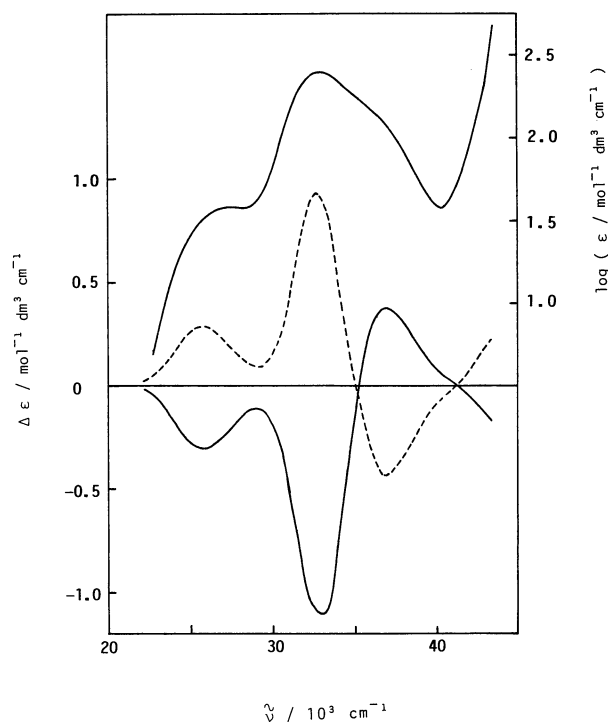


Fig. 3. Absorption spectrum of $\text{S}(\text{N})$ - $[\text{PtCl}_2(\text{R-Hb-Mepn})]$ (**2**) (—), and CD spectra of $\text{S}(\text{N})$ - $[\text{PtCl}_2(\text{R-Hb-Mepn})]$ (**2**) (—), and $\text{R}(\text{N})$ - $[\text{PtCl}_2(\text{R-Hb-Mepn})]$ (**1**) (---), in H_2O containing 0.1 mol dm^{-3} HCl and 0.2 mol dm^{-3} KCl at room temperature.

carbon (C_r) would be weak. Consequently, the CD sign must be attributed to the geometric arrangement around the secondary nitrogen, rather than the nitrogen configuration named according to the general rule.

^1H NMR Spectra. In order to get a detailed solution structure, 400 MHz ^1H NMR spectra of both isomers were recorded using $\text{DCl-D}_2\text{O}$ solution. Under the measurement conditions, H-D exchange proceeded fast at O-H but amino protons were retained so as to give couplings with rest of the molecule. The high-field equipment precludes any detection of the couplings of protons with ^{195}Pt .³⁴⁾ The numerical data of the chemical shifts and coupling constants based on the first-order analysis are listed in Table 7 and methylene and

Table 6. Comparison of Cotton Effects and Structures of $[\text{PtCl}_2\text{L}]$ Complexes

L	Cotton effect		Nitrogen configuration	Chelate ring conformation	Disposition of <i>N</i> -substituent	Octant sign ^{a,b)}		
	$^1\text{A}_1 \rightarrow ^1\text{A}_2$	$^1\text{A}_1 \rightarrow ^1\text{E}$				C_r	C_r	C_N
<i>R</i> -Hb-Mepn	+	—	<i>R</i>	λ	Equatorial	—	—	—
<i>R</i> -Hb-Mepn	—	+	<i>S</i>	δ	Equatorial	+	+	+
<i>S</i> -Me-pn ^{c)}	—	+	<i>R</i>	δ	Equatorial	+	+	+
<i>S</i> -Me-pn ^{c)}	+	—	<i>S</i>	δ	Axial	+	+	—
<i>R</i> -pn ^{d)}	(e)	+		λ		—	—	

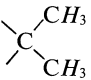
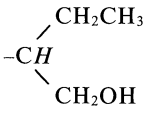
a) Ref. 30. b) C_r and C_N denote chelate ring carbon and carbon atom attached to the nitrogen atom in *N*-substituent.

c) Refs. 3, 4. d) Ref. 26. e) Not observed.

methine region traces are reproduced in Figs. 4 and 5 for **1** and **2** respectively along with those recorded under irradiation at several selected resonances. The two methyl groups bonded to C(2) on the five-membered chelate ring appeared as separated singlets with spacing of ca. 0.153 ppm. The two methylene protons on the five-membered chelate ring appeared as an AB protons which were further splitted by different coupling

constants with the secondary amino protons. The latter coupling is weak for the proton in the higher field (5.2 Hz and 5.3 Hz for **1** and **2**) than that in the lower field (12 Hz and 11.5 Hz for **1** and **2**). This difference shows that the protons appearing at the higher (lower) field is assigned to those with equatorial(axial) dispositions based on the angular dependence of the coupling constant provided the secondary amino proton takes an axial disposition.

Table 7. ^1H Chemical Shifts^{a)} and Coupling Constants^{b)} of *R(N)*- and *S(N)*-[PtCl₂(*R*-Hb-Mepn)]

	1 <i>R(N)</i> -Isomer	2 <i>S(N)</i> -Isomer
$-\text{CH}_2-\text{CH}_3$	0.954 (7.51)	1.050 (7.51)
$-\text{CH}_2-\text{CH}_3$	1.623 (7.5, 10.9, 10.9) 1.811 (7.5, 10.9, 10.9)	1.669 (7.5, 7.5, 10.6) 2.612 (7.5, 7.5, 3.5)
	1.370 (s) 1.521 (s)	1.386 (s) 1.539 (s)
$-\text{C}(\text{CH}_3)_2-\text{CH}_2-\text{NH}$	2.514 (12.6, 5.2, 2.3 ^{c)}) 2.688 (12.1, 12.1)	2.438 (11.5, 5.3, 1.7 ^{c)}) 2.532 (11.5, 11.5)
$-\text{CH}_2-\text{OH}$	4.356 (12.1, 5.0) 4.412 (12.1, 4.4)	3.598 (12.5, 9.7) 3.727 (12.5, 4.0)
	3.225	3.383
$-\text{NH}_2$	5.151 5.218	5.200 5.268
$-\text{NH}$	6.116	5.933

a) Chemical shifts in ppm from internal TSP. b) Coupling constants are found in parentheses in Hz.

c) $^4J(\text{H}-\text{N}-\text{C}(\text{CH}_3)_2-\text{CH})$.

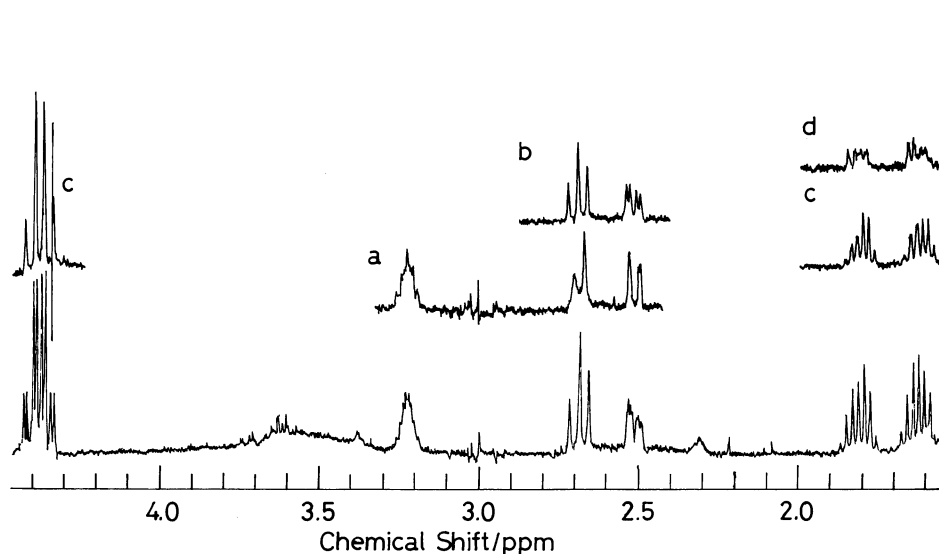


Fig. 4. 400 MHz ^1H NMR spectrum of *R(N)*-[PtCl₂(*R*-Hb-Mepn)] (**1**) in D₂O (containing 0.1 mol dm⁻³ DCl and 0.1 mol dm⁻³ KCl) and double-resonance spectra (a—d) irradiated at (a) $-\text{NH}$ signal ($\delta=6.13$); (b) $-\text{NH}_2$ signal ($\delta=5.22$); (c) the methine signal ($\delta=3.23$); (d) the methyl (in *N*-hydroxybutyl) signal ($\delta=0.95$).

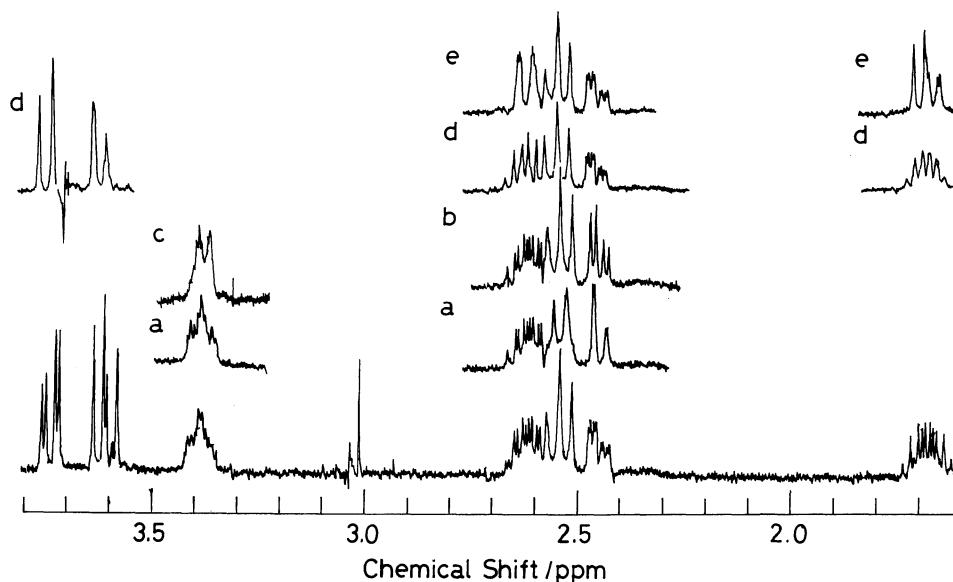


Fig. 5. 400 MHz ^1H NMR spectrum of $S(N)$ -[PtCl $_2$ (*R*-Hb-Mepn)] (**2**) in D $_2$ O (containing 0.1 mol dm $^{-3}$ DCl and 0.1 mol dm $^{-3}$ KCl) and double-resonance spectra (a–e) irradiated at (a) $-\text{NH}$ signal ($\delta=5.93$); (b) $-\text{NH}_2$ signal ($\delta=5.24$); (c) $-\text{CH}_2\text{OH}$ signal (lower field) ($\delta=3.73$); (d) the methine signal ($\delta=3.38$); (e) the methyl (in *N*-hydroxybutyl) signal ($\delta=1.05$).

Furthermore, a long range coupling between the equatorial proton and one of the primary amino protons is observed for each isomer, the long range 4J coupling is operative when the $\text{H}-\text{C}-\text{H}$ segment lies in zig-zag fashion.^{35,36} This requirement enabled us to assign the higher field signal to the equatorial proton for **1** and **2**. In the tetramine type of Pt(II) such as [Pt(NH $_3$) $_2$ (*R*-pn)] $^{2+}$, the axial protons resonates at higher field than the equatorial protons.^{2,37–39}

Significant differences are found in chemical shifts in the *N*-hydroxybutyl side chain. The CH $_3$ CH $_2$ -protons resonate at 1.623 and 1.811 ppm for **1** but at 1.669 and 2.612 ppm for **2**. On the other hand DOCH $_2$ -protons at 4.356 and 4.412 ppm for **1** but at 3.598 and 3.727 ppm for **2**. The down field shift of DOCH $_2$ -protons for **1** and of one of CH $_3$ CH $_2$ -proton for **2** seems to be the reflection of their locations, with respect to the coordination plane revealed by crystallography. The *N*-hydroxybutyl group adopts a configuration of *R*, then the HOCH $_2$ - and CH $_3$ CH $_2$ -group extend in the direction perpendicular to the coordination plane and located in the vicinity of platinum for **1** and **2** respectively, while the CH $_3$ CH $_2$ - and HOCH $_2$ -group takes equatorial disposition and have chemical shifts in normal region for **1** and **2** respectively.

Reversible Inversion at the Coordinated Secondary Amine. The CD intensities of a buffered solution of **1** and **2** gradually changed as the isomerization proceeded. Based on the CD patterns, side reactions occurred but were not so significant for determination of the rate.

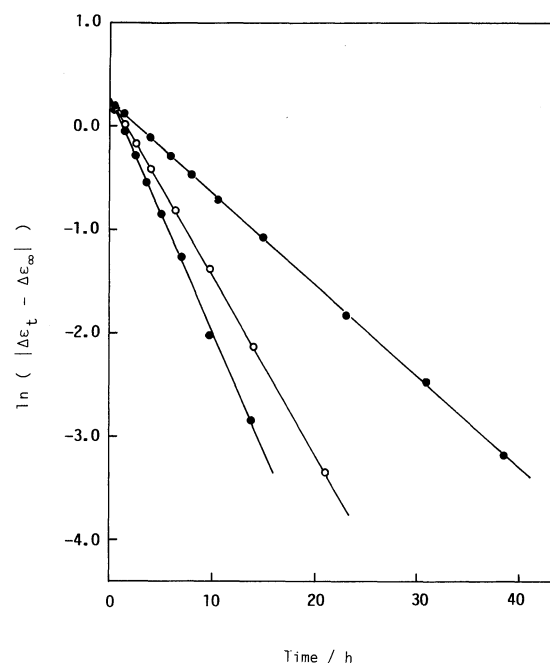


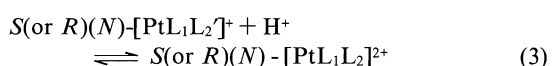
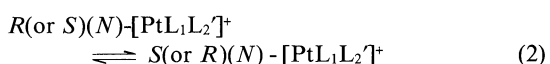
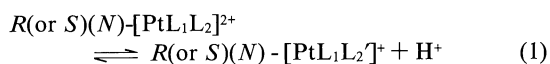
Fig. 6. Plots of $\ln(|\Delta\epsilon_t - \Delta\epsilon_\infty|)$ versus time for the reversible inversion reaction of $R(N)$ -[PtCl $_2$ (*R*-Hb-Mepn)]: (a) pH 4.92, [Complex]= 5.6×10^{-4} mol dm $^{-3}$; (b) pH 5.17, [Complex]= 5.5×10^{-4} mol dm $^{-3}$; (c) pH 5.31, [Complex]= 4.7×10^{-4} mol dm $^{-3}$, [KCl]=0.20 mol dm $^{-3}$, [CH $_3$ COONa]+[CH $_3$ COOH]=0.04 mol dm $^{-3}$, $50.0 \pm 0.1^\circ\text{C}$.

Table 8. Rate Constants for the Inversion Reaction $R(N)$ - $[PtCl_2(R-Hb-Mepn)] \rightleftharpoons S(N)$ - $[PtCl_2(R-Hb-Mepn)]$ and Equilibrium Constants of the Isomers^{a,b)}

pH	$10^5 k_{obsd}/s^{-1}$	$10^{-4} k_i/dm^3 \text{ mol}^{-1} s^{-1}$	K_{eq}
4.92	2.47	5.52	1.9
5.17	4.76	5.99	1.9
5.31	6.34	5.78	2.0

a) In 0.04 M acetate buffer and 0.2 M KCl (1M=1 mol dm^{-3}). b) At 50°C.

For complex **1**, the plot of $\ln(\Delta\epsilon_t - \Delta\epsilon_\infty)$ vs. time gave a straight line for at least three half-lives (Fig. 6). From its slope the pseudo-first-order rate constant, k_{obsd} , which showed pH dependence, was obtained. Almost equal values of k_{obsd} ($2.40 \times 10^{-5} s^{-1}$ (pH 4.92), $4.26 \times 10^{-5} s^{-1}$ (pH 5.17), and $5.33 \times 10^{-5} s^{-1}$ (pH 5.31)) were obtained under the same conditions using complex **2** as the starting material, however, they were relatively uncertain because of its more favorable property at equilibrium. The second-order rate constants, k_i , were calculated by dividing k_{obsd} by $[OH^-]$. The results are summarized in Table 8, therefore, the rate of the reaction for **1** or **2** is expressed by $\text{rate} = k_i[\text{complex}][OH^-]$. For the racemization at an asymmetric nitrogen center in $[PtL_1L_2]^{2+}$, the following mechanism has been proposed,^{6,7)} (for example $L_1 = (NH_3)_2$, $L_2 = CH_3NHCH_2CH_2NH_2$, $L_2' = CH_3NCH_2CH_2NH_2$).



Both deprotonation (1) and reprotonation (3) were established much faster than the inversion (2) process at the nitrogen center. The values obtained here, which were found comparable to that of the related *S*-Me-pn complex, are probably consistent with the above mechanism. The diastereomeric equilibrium constant, $K_{eq} = S(N)/R(N)$, or $[PtCl_2(R-Hb-Mepn)]$ system was found to be in the vicinity of 2, which is considerably larger than that of $[PtCl_2(S-Me-pn)]$.³⁾ For the latter complex this constant was evaluated to be almost 1.

References

- 1) a) F. K. V. Leh and W. Wolf, *J. Pharm. Sci.*, **65**, 315 (1976); b) K. P. Beaumont, C. A. McAuliffe, and M. J. Cleare, *Chem. -Biol. Interact.*, **14**, 179 (1976); c) M. J. Cleare and J. D. Hoeschule, *Bioinorg. Chem.*, **2**, 187 (1973); d) P. Melius and C. A. McAuliffe, *J. Med. Chem.*, **18**, 1150 (1975); e) Z. Simon, M.

Mracec, A. Maurer, S. Poliecec, and C. Dragulescu, *Rev. Roum. Biochim.*, **14**, 117 (1977).

2) T. W. Hambley, C. J. Hawkins, J. Martin, J. A. Palmer, and M. R. Snow, *Aust. J. Chem.*, **34**, 2505 (1981).

3) B. Bosnich and E. A. Sullivan, *Inorg. Chem.*, **14**, 2768 (1975).

4) R. G. Ball, N. J. Bowman, and N. C. Payne, *Inorg. Chem.*, **15**, 1704 (1976).

5) Y. Nakayama, K. Matsumoto, S. Ooi, and H. Kuroya, *Bull. Chem. Soc. Jpn.*, **50**, 2304 (1977).

6) J. B. Goddard and F. Basolo, *Inorg. Chem.*, **8**, 2223 (1976).

7) D. A. Buckingham, L. G. Marzilli, and A. M. Sargeson, *J. Am. Chem. Soc.*, **91**, 5227 (1969).

8) G. M. Searle and E. R. T. Tiekink, *Inorg. Chim. Acta*, **156**, 57 (1989).

9) B. D. Sarma, S. K. Daley, and S. K. Elespuru, *Chem. -Biol. Interact.*, **46**, 219 (1983).

10) See for example: a) R. G. Wilkinson, R. G. Shepherd, J. P. Thomas, and C. O. Baughn, *J. Am. Chem. Soc.*, **83**, 2212 (1961); b) J. P. Thomas, C. O. Baughn, R. G. Wilkinson, and R. G. Shepherd, *Am. Rev. Respir. Dis.*, **83**, 891 (1961); c) R. G. Wilkinson, M. B. Cantrall, and R. G. Shepherd, *J. Med. Pharm. Chem.*, **5**, 835 (1962); d) M. M. Chen, C. S. Lee, and J. H. Perrin, *J. Pharm. Sci.*, **73**, 1053 (1984); e) C. L. Woodley, *J. Clin. Microbiol.*, **23**, 385 (1986).

11) G. Bemski, M. Rieber, and H. Reyes, *FEBS Lett.*, **23**, 59 (1972).

12) A. B. King and R. Schwartz, *J. Nutr.*, **117**, 704 (1987).

13) M. Neamtu and I. Grecu, *Chujul Med.*, **57**, 279 (1984).

14) J. A. Broomhead, *J. Am. Chem. Soc.*, **90**, 4480 (1968).

15) A. Pasini and C. Caldirola, *Inorg. Chim. Acta*, **151**, 19 (1988).

16) T. Tsuji and T. Ueda, *Chem. Pharm. Bull.*, **12**, 946 (1964).

17) SDP Users Guide Version 3.0; Enraf-Nonius and B. A. Frenz and Associates Inc., Delft, Holland, and College Station, TEX, U. S. A., 1985.

18) D. T. Cromer and L. T. Waber, "International Table for X-Ray Crystallography," Kynoch Press, Birmingham, England (1974), Vol. 4.

19) C. K. Johnson, "ORTEP II" Report No. ORNL 5138, Oak Ridge National Laboratory, Oak Ridge, TN (1976).

20) R. Hamalainen, M. Lehtinen, and M. Ahlgren, *Arch. Pharm.*, **318**, 26 (1985).

21) J. Iball, M. MacDougall, and S. Scrimgeour, *Acta Crystallogr., Sect. B*, **31**, 1672 (1975).

22) F. P. Fanizzi, L. Maresca, G. Natile, M. Lanfranchi, A. M. Manotti-Lanfredi, and A. Tiripicchio, *Inorg. Chem.*, **27**, 422 (1988).

23) F. D. Rochon and R. Melanson, *Inorg. Chem.*, **26**, 989 (1987).

24) R. Melanson, C. Chevrotiere, and F. D. Rochon, *Acta Crystallogr., Sect. C*, **43**, 57 (1987).

25) K. Matsumoto, S. Ooi, M. Sakuma, and H. Kuroya, *Bull. Chem. Soc. Jpn.*, **49**, 2129 (1976).

26) H. Ito, J. Fujita, and K. Saito, *Bull. Chem. Soc. Jpn.*, **40**, 2584 (1967).

27) K. Nakayama, T. Komorita, and Y. Shimura, *Bull. Chem. Soc. Jpn.*, **57**, 1336 (1984).

28) E. A. Sullivan, *Can. J. Chem.*, **57**, 67 (1979).

29) C. J. Hawkins and J. Martin, *Inorg. Chem.*, **21**, 1074 (1982).

- 30) C. J. Hawkins and E. Larsen, *Acta Chem. Scand.*, **19**, 185 (1965).
- 31) C. J. Hawkins and E. Larsen, *Acta Chem. Scand.*, **19**, 1915 (1965).
- 32) B. Bosnich and J. M. Harrowfield, *J. Am. Chem. Soc.*, **94**, 3425 (1972).
- 33) S. F. Mason, *J. Chem. Soc. A*, **1971**, 667.
- 34) L. E. Erickson, J. E. Sarneski, and C. N. Reilley, *Inorg. Chem.*, **14**, 3007 (1975).
- 35) V. R. Haddon and L. M. Jackman, *Org. Magn. Reson.*, **5**, 333 (1973).
- 36) J. D. Remijnse, B. G. M. Vandeginste, and B. M. Weps, *Recl. Trav. Chim. Pays-Bas*, **92**, 804 (1973).
- 37) C. J. Hawkins and R. M. Peachey, *Aust. J. Chem.*, **29**, 33 (1976).
- 38) S. Yano, H. Ito, Y. Koike, J. Fujita, and K. Saito, *Bull. Chem. Soc. Jpn.*, **42**, 3184 (1969).
- 39) S. Yano, T. Tukada, M. Saburi, and S. Yoshikawa, *Inorg. Chem.*, **17**, 2520 (1978).
-